

Structural Reliability Evaluation of Ceramic Components

Jyunichi Hamanaka, Akihiko Suzuki, Keiichi Sakai

Ishikawajima-Harima Heavy Industries Co., Ltd.

3-1-15, Toyosu, Koto-ku, Tokyo, 135, Japan

Abstract

A design guide of ceramic components which has been developed in Japanese national project was reviewed. An analytical evaluation method for the effect of proof testing applied to ceramic components has been also proposed. Based on this method, the effectiveness of a proof test can be evaluated even if the loading pattern is different from that in a service condition.

1. Introduction

Structural ceramics usually maintain high strength at elevated temperature and have eminent resistance against erosion. On the contrary, ductility and toughness of ceramics are relatively lower compared to these of metals.

Moreover, critical value of strength data scatters over a wide range. So synthetic approach is necessary for application of ceramics to structural components, that is, methods for strength evaluation, design and assurance must be developed simultaneously. The relationships of these methods are shown in Fig. 1. In this paper, an overview on the design guide for ceramic components developed in Japanese national project is presented and an analytical evaluation method for the proof testing is discussed precisely.

2. Design guide for ceramic components⁽¹⁾

It is necessary to prepare a systematic design guide for wide application of ceramics to various structural components. It does not seem that there

existed any design guide reported. But now, in Japan, a project about research and development of fine ceramics is in progress under the management of the Engineering Research association for high performance ceramics under sponsorship of the Agency of Industrial Science and Technology.

In this project the design guide for ceramic components has been developed. This design guide intends to assure the safety and reliability of ceramic components by keeping the failure probability of the components under an allowable level. In this guide, failure modes such as fast fracture, static fatigue and cyclic fatigue are taken into consideration. Basic design procedure for preventing fast fracture is shown in Fig. 2. Design minimum strength S_u in this figure is determined by the average tensile strength and Weibull parameter. β and γ are design factors relating to stress distribution effect and volume effect. K_1 is safety factor relating to the allowable failure probability. In Fig. 3, the basic design procedure for preventing fatigue fracture is schematically shown. S_t in this figure is determined by design fatigue curve corresponding to design usage life.

3. Proof testing of ceramic components

The following methods can be considered to assure the integrity and reliability of ceramic components.

- (1) Proof testing
- (2) Fracture testing of small sized samples of the components
- (3) Nondestructive inspection
- (4) Combination of the above mentioned methods

Among these methods, proof testing is most reliable to assure the integrity of ceramic manufactures. In this chapter, a newly proposed method to evaluate the effect of proof testing is examined.

3.1 Fast fracture strength after proof testing⁽²⁾

In uniaxial stress state, the failure probability of a ceramic component which have endured the proof testing is given as

$$P_p(\sigma_N) = \begin{cases} \frac{P(\sigma_N) - P(\sigma_p)}{1 - P(\sigma_p)} & \text{----- } \sigma_N \geq \sigma_p \\ 0 & \text{----- } \sigma_N < \sigma_p \end{cases} \quad \text{----- (1)}$$

where $P(\sigma)$ means failure probability of components before the proof testing. σ_N and σ_p are nominal stress and proof testing stress, respectively.

For evaluating the effect of proof testing in multiaxial and nonuniform stress state, the followings are assumed:

- (1) Penny shaped flaws are uniformly distributed in a ceramic component (Fig. 4)
- (2) The flaw surface direction is randomly oriented
- (3) Existence probability of a crack whose size is larger than a , $P(a)$, is expressed as

$$P(a) = 1 - \exp \left\{ - \left(\frac{a_0}{a} \right)^{\frac{m}{2}} \cdot \frac{V}{V_0} \right\} \quad \text{----- (2)}$$

where a : flaw size

a_0, V_0 : reference flaw size and reference volume

- (4) Employing the energy release rate criterion for fracture rule, equivalent normal stress Z is expressed as $Z = \{\sigma_n^2 + 4\tau_n^2 / (2 - \nu)^2\}^{\frac{1}{2}}$, where σ_n and τ_n are normal and shear stress acting on the flaw surface (Fig. 4).

3.1.1 Proof test whose loading pattern is similar to that in service condition

In the case of proof testing whose loading pattern is similar to that in service condition, the probability of fast fracture after proof testing can be

obtained by Eq. (1). Assuming that strength distribution of fast fracture is given by two parameter Weibull distribution in uniaxial tension, $P(\sigma_N)$ in Eq.(1) is represented as

$$P(\sigma_N) = 1 - \exp \left\{ -\xi \cdot \sigma_N^m \cdot \int_V \int_0^{\frac{\pi}{2}} \int_0^{\frac{\pi}{2}} \left(\frac{Z}{\sigma_N} \right)^m \cdot y(\sigma_n \cdot 0) \cdot \sin\phi \cdot d\phi \cdot d\theta \cdot dv \right\} \quad \text{----- (3)}$$

where

$$\xi = \frac{1}{\Omega} \cdot \Gamma\left(\frac{1}{m} + 1\right)^m \cdot \left(\frac{\sigma_N}{\sigma_{ref}}\right)^m \cdot \left(\frac{1}{V_{ref}}\right)^{\frac{2}{m}}$$

$$\Omega = \frac{2}{\pi} \cdot \int_0^{\frac{\pi}{2}} \int_0^{\frac{\pi}{2}} \left[\cos^4\phi + \frac{4}{(2-\nu)^2} \cdot (\cos^2\phi - \cos^4\phi) \right]^{\frac{m}{2}} \cdot \sin\phi \, d\phi \, d\theta$$

m : Weibull parameter

σ_N : Nominal stress

$\bar{\sigma}_{ref}$: Average tensile strength using test specimen of volume V_{ref}

$y(\sigma_n \cdot 0)$: Heaviside step function

3.1.2 Proof test whose loading pattern is different from that in service condition

In case of proof testing whose loading pattern is different from that in service condition, Eq.(1) is not available. So, we consider a flaw in small element ΔV_i , whose direction is oriented to the angle ϕ, θ as shown in Fig. 4. Then, equivalent normal stress Z of such flaw is constant in proof testing and in service condition. Namely, the failure probability of a such flaw which has endured proof testing can be expressed as

$$P_{p, \Delta ij}(\sigma_N) = \begin{cases} \frac{P_{\Delta ij}(\sigma_N) - P_{\Delta ij}(\sigma_p)}{1 - P_{\Delta ij}(\sigma_p)} & \text{--- } Z_{A, ij} \geq Z_{p, ij} \\ 0 & \\ & \text{--- } Z_{A, ij} < Z_{p, ij} \end{cases} \quad \text{--- (4)}$$

, where subscript Δij means the value according to the flaw in ΔV_i , of which surface direction is oriented to the angle ϕ, θ . $Z_{A, ij}$ and $Z_{p, ij}$ are the equivalent normal stresses of the flaw in ΔV_i whose surface direction is oriented to the angle ϕ, θ in service and proof testing condition, respectively. $P_{\Delta ij}(\sigma_N)$ in Eq.(4) is written as follows.

$$P_{\Delta ij}(\sigma_N) = 1 - \exp \left\{ -\xi^* \cdot Z_{A, ij}^m \cdot y(\sigma_{nA}, 0) \cdot \sin\phi \cdot \Delta\phi \cdot \Delta\theta \cdot \Delta V \right\} ; \quad \xi^* = \frac{\xi}{8}$$

Then reliability of the above mentioned flaw is given by

$$R_{p, \Delta ij}(\sigma_N) = \begin{cases} \frac{1 - P_{\Delta ij}(\sigma_N)}{1 - P_{\Delta ij}(\sigma_p)} & \text{--- } Z_{A, ij} \geq Z_{p, ij} \\ 1 & \\ & \text{--- } Z_{A, ij} < Z_{p, ij} \end{cases} \quad \text{--- (5)}$$

By considering all flaws in ΔV_i , the reliability of the small element ΔV_i which has endured proof testing is obtained as

$$R_{p, \Delta i}(\sigma_N) = \prod_j R_{p, \Delta ij}(\sigma_N) = \frac{\prod_{Z_{A, ij} \geq Z_{p, ij}} \left\{ 1 - P_{\Delta ij}(\sigma_N) \right\}}{\prod_{Z_{A, ij} \geq Z_{p, ij}} \left\{ 1 - P_{\Delta ij}(\sigma_p) \right\}} \quad \text{----- (6)}$$

where

$$\begin{aligned} \prod_{Z_{A, ij} \geq Z_{p, ij}} \left\{ 1 - P_{\Delta ij}(\sigma_N) \right\} &= \prod_{\text{all } \phi, \theta} \exp \left\{ -\xi^* \cdot Z_{A, ij}^m \cdot \right. \\ &\quad \left. y(\sigma_{nA} \cdot 0) \cdot y(Z_A - Z_p \cdot 0) \cdot \sin \phi \Delta \phi \Delta \theta \cdot \Delta V \right\} \\ &= \exp \left\{ -\xi^* \cdot \sum_{\text{all } \phi, \theta} Z_{A, ij}^m \cdot y(\sigma_{nA} \cdot 0) \cdot y(Z_A - Z_p \cdot 0) \cdot \sin \phi \Delta \phi \Delta \theta \cdot \Delta V \right\} \end{aligned}$$

Taking $\Delta \phi$, $\Delta \theta$ very small, the above equation can be expressed as follows.

$$\begin{aligned} \prod_{Z_{A, ij} \geq Z_{p, ij}} \left\{ 1 - P_{\Delta ij}(\sigma_N) \right\} &= \exp \left\{ -\xi \cdot \int_0^{\frac{\pi}{2}} \int_0^{\frac{\pi}{2}} Z_{A, i}^m \cdot \right. \\ &\quad \left. y(\sigma_{nA} \cdot 0) \cdot y(Z_A - Z_p \cdot 0) \cdot \sin \phi d\phi d\theta \cdot \Delta V \right\} \end{aligned}$$

By substituting $Z_{p,i}$ and σ_{np} into $Z_{A,i}$ and σ_{nA} in the above equation, the denominator in Eq.(6) can be obtained. Where $Z_{p,i}$ and $Z_{A,i}$ are the equivalent normal stresses of Δi in proof testing and in service condition, respectively.

Finally, by applying the weakest link theory to the component which is the assembly of the small element ΔV_i , the reliability of the ceramic components is given by

$$R_p(\sigma_N) = \prod_{\text{all } \Delta i} R_{p, \Delta i}(\sigma_N) = \frac{R_{p1}}{R_{p2}} \quad \text{----- (7)}$$

where

$$R_{P1} = \exp \left\{ -\xi \int_V \int_0^{\frac{\pi}{2}} \int_0^{\frac{\pi}{2}} Z_A^m \cdot y(\sigma_{nA} \cdot 0) \cdot y(Z_A - Z_P \cdot 0) \cdot \sin\phi \cdot d\phi \cdot d\theta \cdot dv \right\}$$

$$R_{P2} = \exp \left\{ -\xi \int_V \int_0^{\frac{\pi}{2}} \int_0^{\frac{\pi}{2}} Z_P^m \cdot y(\sigma_{nP} \cdot 0) \cdot y(Z_A - Z_P \cdot 0) \cdot \sin\phi \cdot d\phi \cdot d\theta \cdot dv \right\}$$

Then, the failure probability of a component which has endured proof testing is obtained by subtracting $R_p(\sigma_N)$ from 1.

3.1.3 Fast fracture by bending test

For verification of the above mentioned theory, bending test was carried out using sintered Si_3N_4 test specimens. Proof test loading was applied by four point bending. The test specimens having endured this proof testing were fractured by three point bending.

Dimensions of the test specimen and loading patterns are shown in Fig. 5. The calculated and experimental results of the fracture strength after proof testing are shown in Fig. 6. These results shows fairly good agreement.

3.2 Fatigue strength after proof testing⁽³⁾

3.2.1 Static fatigue strength after proof testing

Crack propagation rate under uniaxial stress state is assumed to be represented as

$$\frac{da}{dt} = BK_I^n, \quad K_I = C\sigma\sqrt{a} \quad \text{--- (8)}$$

where σ , a , C are applied stress, crack size parameter and the coefficient depending on the crack shape and loading pattern respectively. By integrating Eq.(8), the static fatigue life t_f is obtained as

$$t_f = \zeta(\sigma) \cdot \left[\left\{ \frac{1}{a_i} \right\}^{\frac{n-2}{2}} - \left\{ \frac{1}{a_c(\sigma)} \right\}^{\frac{n-2}{2}} \right] \quad \text{----- (9)}$$

where $a_i, a_c(\sigma)$ are initial and critical flaw size respectively. $\zeta(\sigma)$ is

$$\zeta(\sigma) = \frac{2}{(n-2) \cdot B \cdot C^n \cdot \sigma^n} \quad \text{----- (10)}$$

When proof testing stress and applied stress are expressed as σ_p and σ_A , minimum life t_p assured by proof testing is given by

$$t_p = \zeta(\sigma_A) \cdot \left[\left\{ \frac{1}{a_p} \right\}^{\frac{n-2}{2}} - \left\{ \frac{1}{a_c(\sigma_A)} \right\}^{\frac{n-2}{2}} \right] \quad \text{----- (11)}$$

where a_p is the maximum existing flaw size remaining after proof testing and given by $K_{IC}^2 / (C^2 \sigma_p^2)$. In uniaxial stress state, the static fatigue failure probability after proof testing is given by

$$P_p(t_f) = \begin{cases} \frac{P(t_f) - P(t_p)}{1 - P(t_p)} & \text{---- } t_f \geq t_p \\ 0 & \text{---- } t_f < t_p \end{cases} \quad \text{---- (12)}$$

If proof test loading pattern is similar to that in service condition, the static fatigue failure probability in multiaxial stress state approximately can be expressed as Eq.(12). In this case, minimum assured life t_p of a component in Eq.(12) is calculated by

$$t_p = \zeta(Z_{A, max}) \cdot \left[\left\{ \frac{1}{a_p} \right\}^{\frac{n-2}{2}} - \left\{ \frac{1}{a_c} \right\}^{\frac{n-2}{2}} \right] \quad \text{----- (13)}$$

where $Z_{A,max}$, a_p and a_c are the maximum equivalent normal stress in the service condition, $K_{IC}^2/(C^2 \cdot Z_{p,max}^2)$ and $K_{IC}^2/(C^2 \cdot Z_{A,max}^2)$. And $P(t_f)$ in Eq.(12) is represented as

$$P(t_f) = 1 - \exp \left\{ -\xi \cdot \int_V \int_0^{\frac{n}{2}} \int_0^{\frac{n}{2}} (\eta \cdot t_f \cdot Z_A^n + Z_A^{n-2})^{m^*} \cdot y(\sigma_{nA} \cdot 0) \cdot \sin\phi d\phi d\theta dv \right\} \quad \text{--- (14)}$$

where η and m^* are $(n-2) \cdot B \cdot K_{IC}^{n-2} \cdot C^2/2$ and $m/(n-2)$.

Next, let us examine the effect of proof teting on static fatigue strength in case where loading pattern between proof testing and service condition are different.

As discussed in the item 3.1.2, we consider a flaw in small element ΔV_i whose surface direction is oriented to the angle ϕ , θ as shown in Fig. 4. Minimum life of this flaw assured by proof testing, $t_{p,ij}$, is given by

$$t_{p,ij} = \zeta(Z_{A,ij}) \cdot \left[\left(\frac{1}{a_{p,ij}} \right)^{\frac{n-2}{2}} - \left(\frac{1}{a_{c,ij}} \right)^{\frac{n-2}{2}} \right] \cdot y(\sigma_{np,ij} \cdot 0) \cdot y(Z_{p,ij} - Z_{A,ij} \cdot 0) \quad \text{--- (15)}$$

where $\sigma_{np,ij}$, $a_{p,ij}$ and $a_{c,ij}$ are normal stress to the flaw surface in proof testing condition, $K_{IC}^2/C^2(Z_{p,ij})^2$ and $K_{IC}^2/C^2(Z_{A,ij})^2$. Then, static fatigue probability of this flaw which has endured proof testing is obtained as

$$P_{p,ij}(t_f) = \begin{cases} \frac{P_{ij}(t_f) - P_{ij}(t_{pij})}{1 - P_{ij}(t_{pij})} & \text{--- } t_f \geq t_{pij} \\ 0 & \text{--- } t_f < t_{pij} \end{cases} \quad \text{--- (16)}$$

where $P_{ij}(t_f)$ is

$$P_{ij}(t_f) = 1 - \exp \left\{ -\xi^* \cdot (\eta \cdot t_f \cdot Z_{A,ij}^n + Z_{A,ij}^{n-2})^m \cdot y(\sigma_{nA} \cdot 0) \cdot \sin \phi \Delta \phi \Delta \theta \Delta V_i \right\} \quad \text{--- (17)}$$

$P_{ij}(t_{pij})$ is obtained by substituting t_{pij} into t_f in Eq.(17). The reliability that this flaw doesn't fail within t_f is written as

$$R_{p,ij}(t_f) = \begin{cases} \frac{1 - P_{ij}(t_f)}{1 - P_{ij}(t_{pij})} & \text{--- } t_f \geq t_{pij} \\ 1 & \text{--- } t_f < t_{pij} \end{cases} \quad \text{--- (18)}$$

By considering all flaws in ΔV_i , the reliability of the small element ΔV_i which has endured proof testing is obtained as

$$R_{p,i}(t_f) = \frac{\prod_{t_f \geq t_{pij}} \{1 - P_{ij}(t_f)\}}{\prod_{t_f \geq t_{pij}} \{1 - P_{ij}(t_{pij})\}} \quad \text{--- (19)}$$

where $\prod_{t_f \geq t_{pij}}$ means that products for the limited number of flaws in a condition $t_{pij} \leq t_f$.

Using Heaviside step function $y(t_f - t_{pij} \cdot 0)$, the numerator in Eq.(19) is represented as

$$\prod_{t_f \geq t_{pij}} \left\{ 1 - P_{ij}(t_f) \right\} = \prod_{all \phi, \theta} \exp \left\{ -\xi^* \cdot (\eta \cdot t_f \cdot Z_{A,ij}^n + Z_{A,ij}^{n-2})^{m^*} \cdot y(\sigma_{nA} \cdot 0) \cdot y(t_f - t_{pij} \cdot 0) \cdot \sin \phi \Delta \phi \Delta \theta \cdot \Delta V_i \right\}$$

$$= \exp \left\{ -\xi^* \sum_{all \phi, \theta} \left(\eta \cdot t_f \cdot Z_{A,ij}^n + Z_{A,ij}^{n-2} \right)^{m^*} \cdot y(\sigma_{nA} \cdot 0) \cdot y(t_f - t_{pij} \cdot 0) \cdot \sin \phi \Delta \phi \Delta \theta \cdot \Delta V_i \right\}$$

Taking $\Delta \phi$, $\Delta \theta$ very small, the above equation can be expressed as

$$\prod_{t_f \geq t_{pij}} \left\{ 1 - P_{ij}(t_f) \right\} = \exp \left\{ -\xi \cdot \int_0^{\frac{\pi}{2}} \int_0^{\frac{\pi}{2}} (\eta \cdot t_f \cdot Z_{A,i}^n + Z_{A,i}^{n-2})^{m^*} \cdot y(\sigma_{nA} \cdot 0) \cdot y(t_f - t_{pij} \cdot 0) \cdot \sin \phi d\phi d\theta \cdot \Delta V_i \right\} \quad \text{----- (20)}$$

where $Z_{A,i}$ is equivalent nominal stress of ΔV_i in service condition. By substituting t_{pij} into t_f in Eq.(20), the denominator in Eq.(19) can be obtained. By applying the weakest link theory to the component itself which is an assembly of the small elements, reliability of the component is

$$R_p(t \leq t_f) = \prod_{all \Delta_i} R_{p,i}(t_f) = \frac{R_{p1}}{R_{p2}} \quad \text{----- (21)}$$

where R_{p1} and R_{p2} are represented as

$$R_{p1} = \exp \left\{ -\xi \int_V \int_0^{\frac{\pi}{2}} \int_0^{\frac{\pi}{2}} (\eta \cdot t_f \cdot Z_A^n + Z_A^{n-2})^{m^*} \cdot y(\sigma_{nA} \cdot 0) \cdot y(t_f - t_{pij} \cdot 0) \cdot \sin \phi d\phi d\theta \cdot \Delta V_i \right\}$$

$$R_{p2} = \exp \left\{ -\xi \int_V \int_0^{\frac{n}{2}} \int_0^{\frac{n}{2}} (\eta \cdot t_{pij} \cdot Z_A^n + Z_A^{n-2})^{m*} \cdot y(\sigma_{nA} \cdot 0) \cdot y(t_f - t_{pij} \cdot 0) \cdot \sin\phi d\phi d\theta \cdot dv \right\}$$

Then the failure probability of a component during the life time t_f is obtained as

$$P_p(t_f) = \begin{cases} 1 - R_p(t \leq t_f) & \text{--- } t_f \leq t_p^* \\ 0 & \text{--- } t_f > t_p^* \end{cases}$$

----- (22)

where t_p^* is the minimum value of t_{pij} .

3.2.2 Reliability analysis of turbine disk

In order to verify the above mentioned theory, reliability analysis of a gas turbine disk was performed. Analysis model of the gas turbine disk is shown in Fig. 7. Heat transfer condition is shown in the same figure. Centrifugal force and thermal loading due to gas flow are applied to the disk. The disk material is hot pressed silicon nitride, and its thermal conductivity, specific heat, and specific gravity are $19W/(m \cdot k)$, $0.92KJ/(kg \cdot k)$ and $3.26 \times 10^3 kg/m^3$. Young's modulus, Poisson's ratio, and linear expansion are $3 \times 10^5 MPa$, 0.27 and $3.7 \times 10^{-6}/^\circ C$. For the Weibull parameter, σ_{ref} , V_{ref} and K_{IC} , we use 9.0 , $760 MPa$, $8600 mm^3$ and $3.1 MPa^{1/2}$. Values of C , B , and n in Eq.(8) are 1.13 , $2.8 \times 10^{-1.3} (m, sec, MPa)$ and 15 . The rotating speed in a service condition is $30,000 rpm$. Calculated results of the failure probability due to centrifugal force is shown in Fig. 8.

In this figure, solid line is the calculated results for the rotating speed 30,000 rpm without proof testing. On the other hand, dotted line and chained line are calculated results in case where the disk endured 50,000 rpm proof testing. Dotted line is calculated results by Eq.(12) and Eq.(14). Chained line is calculated results by Eq.(22). Eq.(12) can be used for this example, because the loading pattern of proof testing is similar to that in service condition. But the effect of proof testing can not be seen in the results expressed by dotted line. It is explained by the fact that t_p in Eq.(12) is so small (≈ 0.02 sec) that $P(t_p)$ in Eq.(12) is almost zero and $P_p(t_f)$ is almost $P(t_f)$. In the analysis of chained line, the minimum assured life t_{pij} is determined for every elements and every flaws. So, the effect of proof testing can be seen in the results expressed by chained line.

Calculated results of the failure probability due to centrifugal force and thermal loading are shown in Fig. 9. In this figure, failure probability without proof testing is expressed by solid line and that with 50,000 rpm proof testing is expressed by chained line. Fig. 9 shows the static fatigue life of gas turbine disk can be extended by proof testing whose loading pattern is different from that in service condition.

3.2.3 Cyclic fatigue strength after proof testing

As the mechanism of cyclic fatigue fracture, the following two types of fracture can be considered.

- (1) Time depending fracture
- (2) Cyclic depending fracture

The time depending fracture in cyclic fatigue can be evaluated by the slow crack growth under a varying load. Then the effect of proof testing can be evaluated by applying the above mentioned theory about static fatigue.

In the case of cyclic depending fracture, it can be considered that the fatigue fracture is caused by cyclic depending crack growth from the initial flaws.

The crack growth rate is assumed as follows:

$$\frac{da}{dN} = B \left\{ K_{max} (1 - \alpha R) \right\}^n \quad \text{--- (23)}$$

where K_{max} and R are maximum stress intensity factor and stress ratio, respectively. Then the effect of proof testing can be evaluated by replacing t_f , $P(t_f)$, $P_p(t_f)$, t_{pij} , B , $Z_{A,ij}$ in Eq.(12), Eq.(22) by N_f , $P(N_f)$, $P_p(N_f)$, N_{pij} , $B(1 - \alpha R)^n$ and $(Z_{A, ij})_{max}$, respectively. Test results by four point bending are shown in Fig. 10 with the average life estimated by the above mentioned theory. Agreement between the test results and calculated results is observed.

4. Conclusion

Design method and assurance method of structural ceramic components are discussed. Especially, a new evaluation method for the effect of the proof testing is proposed in case where loading pattern is different from that in service condition. A part of this work was performed under the contract between the Agency of Industrial Science and Technology of MITI and the Engineering Research Association for High Performance Ceramics, as a part of R&D Project of Basic Technology for Future Industries.

References

- (1) Suzuki, A., et al, Trans JSME, A, 53-495 (1987), 2134
- (2) Hamanaka, J., et al, Trans JSME, A, 53-492 (1987), 1638
- (3) Hamanaka, J., et al, Trnas JSME, A, to be submitted

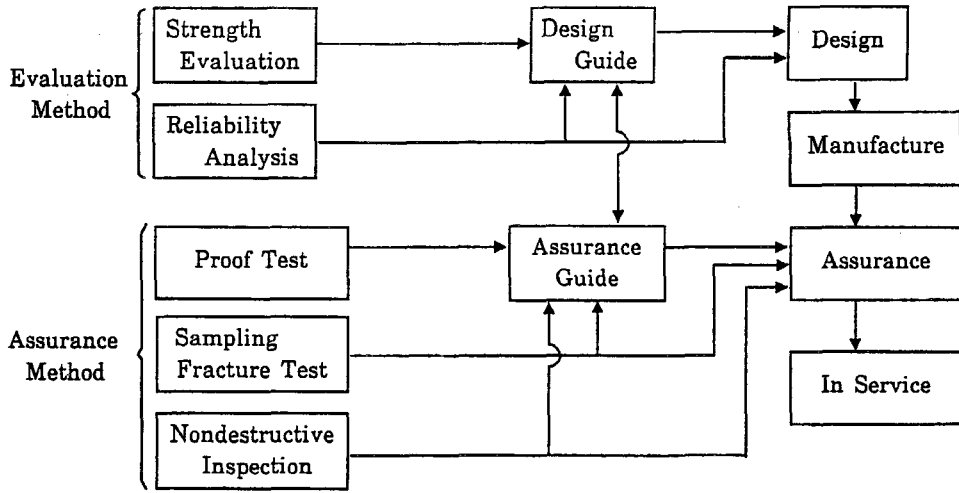


Fig. 1 Design and integrity assurance of ceramic component

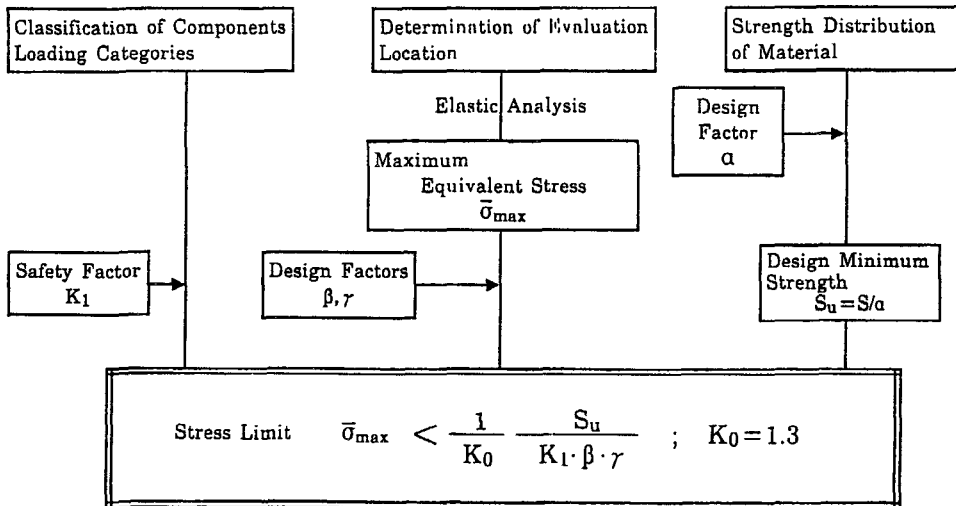


Fig. 2 Design procedure for preventing fast fracture

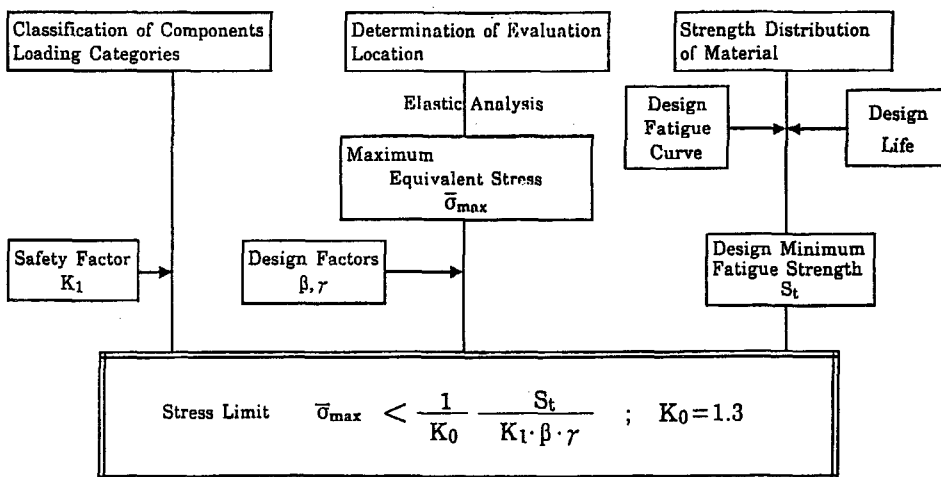


Fig. 3 Design procedure for preventing fatigue fracture

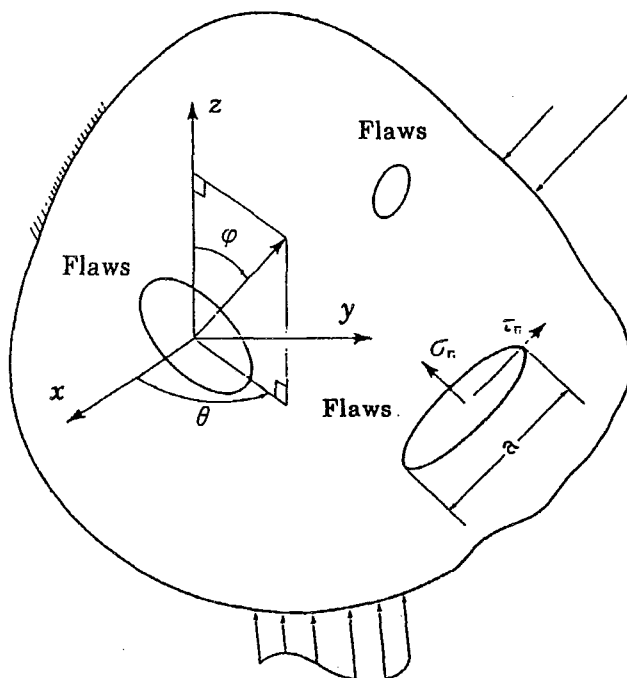


Fig. 4 Flaws in ceramic component

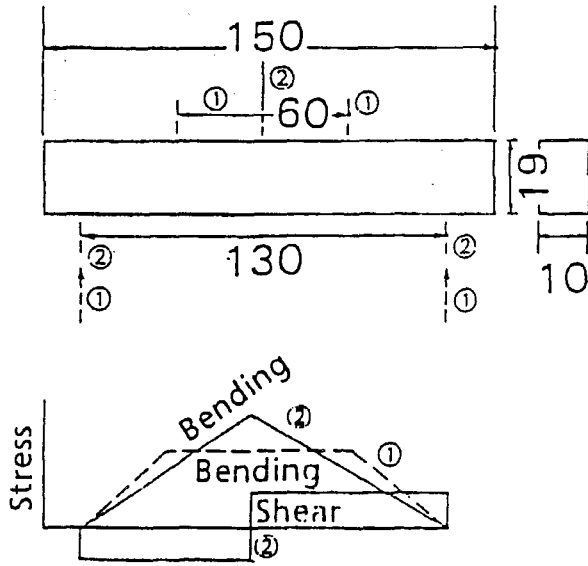


Fig. 5 Bending test specimen and loading pattern

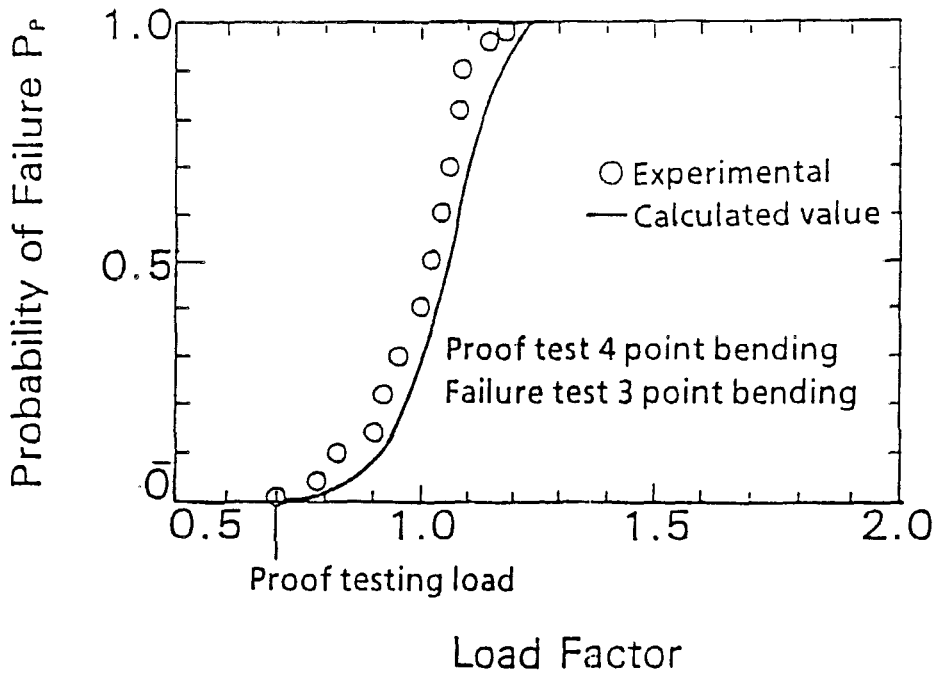


Fig. 6 Bending test results and calculated value

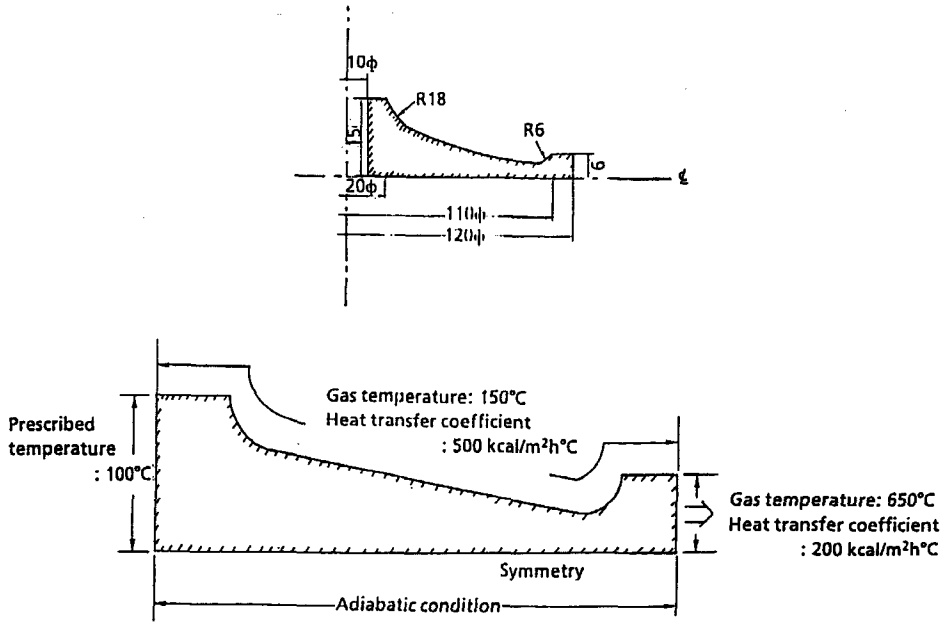


Fig. 7 Analysis model of gas turbine disk

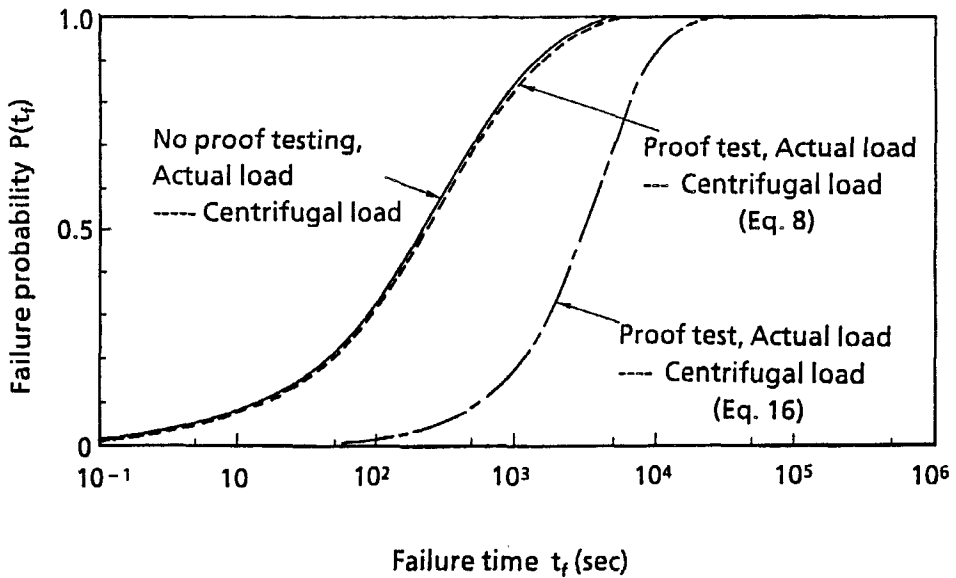


Fig. 8 Failure probability of turbine disk due to centrifugal loading

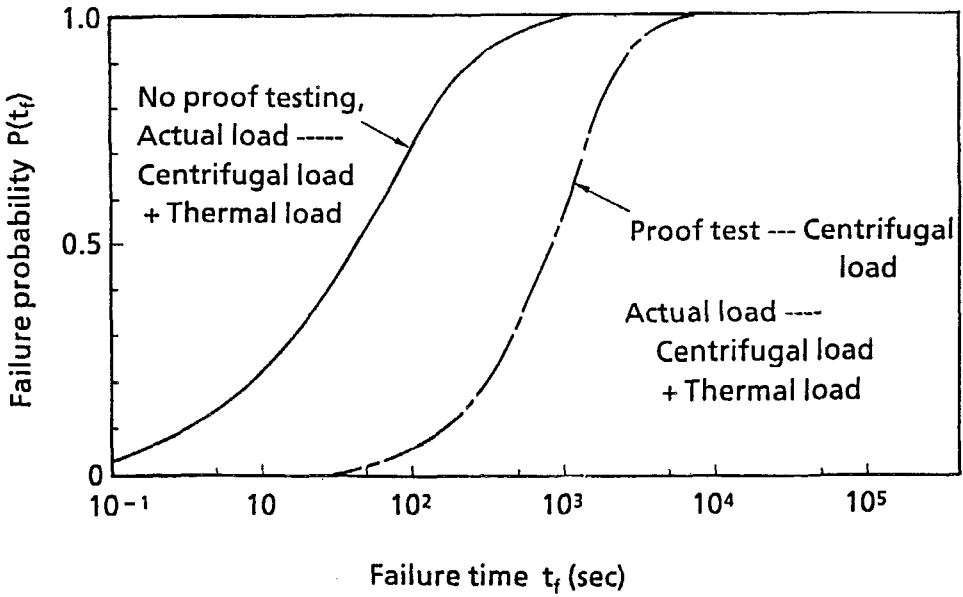


Fig. 9 Failure probability of turbine disk due to centrifugal and thermal loadings

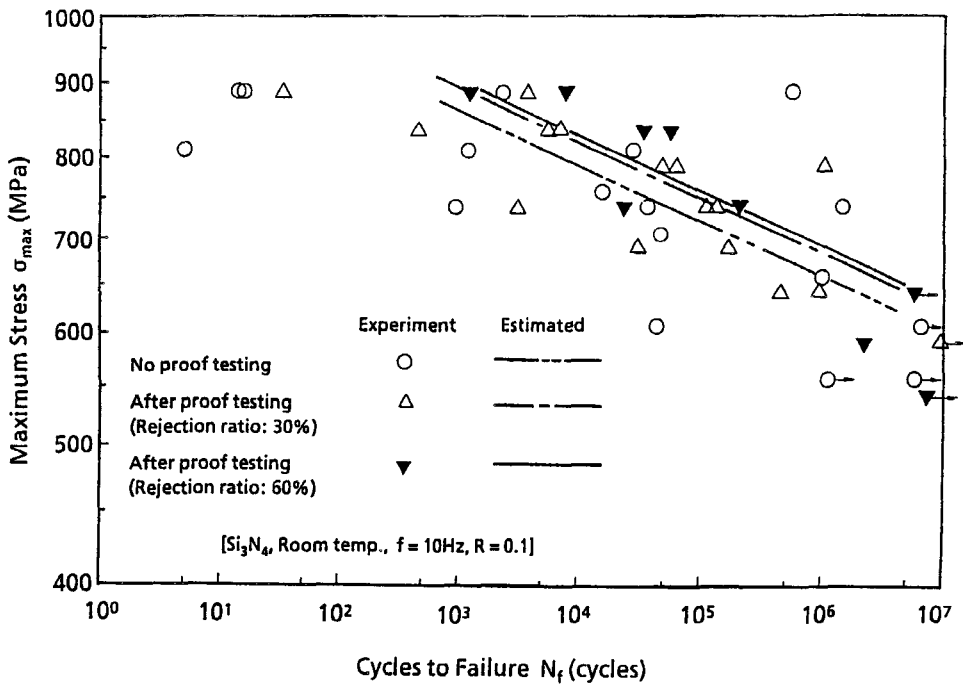


Fig. 10 Cyclic fatigue strength after proof testing